

Dissipation of Oscillation Energy and Distribution of Damping Power in a Multimachine Power System: A Small-signal Analysis

Kaustav Chatterjee, *Student Member, IEEE* and Nilanjan Ray Chaudhuri, *Senior Member, IEEE*

Abstract—This paper revisits the concept of damping torque in a multimachine power system and its relation to the dissipation of oscillation energy in synchronous machine windings. As a multimachine extension of an existing result on a single-machine-infinite-bus (SMIB) system, we show that the total damping power for a mode stemming from the interaction of electromagnetic torques and rotor speeds is equal to the sum of average power dissipations in the generator windings corresponding to the modal oscillation. Further, counter-intuitive to the SMIB result, we demonstrate that, although the equality holds on an aggregate, such is not the case for individual machines in an interconnected system. To that end, distribution factors are derived for expressing the average damping power of each generator as a linear combination of average powers of modal energy dissipation in the windings of all machines in the system. These factors represent the distribution of damping power in a multimachine system. The results are validated on IEEE 4-machine and 16-machine test systems.

Index Terms—Damping torque, damping power, multimachine system, oscillation energy dissipation, synchronous machines

I. INTRODUCTION

IN small-signal analysis, stability of a power system under electromechanical oscillations is determined by studying the eigenvalues of the system linearized around the quasi-steady-state operating point or by performing modal estimation on the response variables. In either case, the damping ratios obtained indicate the margin of system stability, but do not quantify the damping contribution from individual sources. In that regard, the small-signal representation of a generator's electromagnetic torque as a phasor in its synchronously rotating rotor speed-angle reference frame offers geometric intuition into decomposing the torque into its damping and synchronizing components. Conceptualized by Park in his 1933 paper [1] and furthered by Concordia [2], [3], Shepherd [4], and notable others [5]–[9], the damping and synchronizing torque coefficients contribute towards insightful understanding of the stabilizing contributions coming from the machine and its associated governor and excitation systems. Consequently, some of the early designs of power system stabilizers for damping oscillations have evolved out of these notions. However, historically, these studies on damping torque have been presented either considering a SMIB system or by reducing the system to a linearized single-machine equivalent. Unlike a SMIB system, damping torque of a generator in a multimachine system depends not only on its own speed-deviation but

also on that of the other machines, their excitation systems, and the overall network structure and parameters. Also, the analytical modeling of these differ in literature, for instance, authors in [10] model damping torque as a higher degree polynomial in speed-deviations, in contrast to linear terms in [11]. The 1999 IEEE task force report investigating modeling adequacy for representing damping in multimachine stability studies [12] identified eight different sources of damping and recommended abstracting their contributions into a single retarding torque in the swing equation of each generator.

Damping torque, thus, over the years, has largely remained a *conceptual* tool for analyzing stability in power systems. Although some of the initial works listed before highlighted an *intuitive* link between damping torque and dissipation of oscillation energy, it is only in the recent works [13] and [14] that a rigorous mathematical connection between the two has been established for a SMIB system. However, for multimachine systems such a connection is yet to be confirmed – in this paper, we make a maiden attempt to fill this gap. To that end, we use a simplified mathematical model for multimachine systems to establish an equivalence between the average power dissipation due to the damping torques on the rotors and the average rates of oscillation energy dissipation in the machine windings. In this context, we make a note of [15], where claims regarding the consistency of damping and dissipation coefficients in multimachine systems are made based on presupposition of this equality without any formal proof. Going ahead, in the paper we also demonstrate that the damping power of each machine stemming from the interaction of its own speed and torque, is derived in parts from the rates of energy dissipation in the windings of all machines, over and above it's own winding.

At this point, it is important to clarify that the focus of this paper is not on improving the algorithmic tools of [14] or [13] for perfecting the science of locating oscillation sources or to present an alternate path for doing the same, but to derive further analytical insights from the findings of these two seminal papers. Our primary intention is to bridge a mathematical connection between the concept of transient energy dissipation, as introduced in [14], and the notion of damping torque, which is nearly a century old.

The contributions of the paper are as follows: (1) we develop a phasor-based small-signal-formulation for calculating the mode-wise average powers (i.e. damping powers) of electromechanical oscillation due to the interaction of damping torque and speed in each machine; (2) using this framework for a simplified system model with lossless transmission network and constant power loads, we extend the SMIB results in [14]

K. Chatterjee and N. R. Chaudhuri are with The School of Electrical Engineering and Computer Science, The Pennsylvania State University, University Park, PA 16802, USA (e-mail: kuc760@psu.edu; nuc88@psu.edu)

Financial support from the NSF grant under award CNS 1739206 is gratefully acknowledged.

to show that the total damping power for a mode is equal to the sum of average power dissipations in the generator windings corresponding to the modal oscillation; and finally, (3) counter-intuitive to the SMIB result in [14], we demonstrate that the aforementioned equality does not hold for individual machines in an interconnected system – in fact the damping power in each machine can be expressed as a weighted linear combination of power dissipation in windings of different generators. These weighing factors (called ‘distribution factors’ in the paper) are analytically derived – which essentially describe the participation of the power dissipation in different machines in constituting the damping power of each generator.

To that end, in the next section, we derive a linearized representation of the simplified system mentioned earlier with a third-order synchronous generator model. Building on this model, we present contributions (1)–(3) in Sections III–V, which are followed by case studies on IEEE 4-machine and 16-machine test systems in Section VI to validate the claims – both for the simplified model used in derivation, and for systems with detailed machine models. Finally, concluding remarks are presented in Section VII.

Notations: Superscripts T , $*$, and H are respectively the transpose, conjugate, and Hermitian operators. $\Re\{\cdot\}$ and $\Im\{\cdot\}$ denote the real and imaginary parts of a complex entity.

II. SIMPLIFIED SYSTEM MODEL: LINEARIZED REPRESENTATION

Consider a n -bus transmission system of which, without loss of generality, first n_g are designated as generator buses. The network is lossless and each synchronous generator is described by a third-order machine model capturing the electromechanical dynamics of the rotor and the field flux. In addition, assume manual excitation for the generators and constant power loads at all buses.

The differential equations describing the dynamics of each generator are same as those given in eqns (6.132) – (6.134) of [11]. Further, the stator and network algebraic equations can be obtained from eqns (6.142) – (6.144). Since we assume a lossless network, in eqns (6.143) and (6.144) of [11], $\alpha_{ik} = \pi/2$ for $i \neq k$, and $\alpha_{ii} = -\pi/2$. Unless specified otherwise, all symbols have their usual meanings as in [11].

We eliminate the stator algebraic equations by substituting I_{d_i} and I_{q_i} obtained from eqn (6.142) into eqns (6.143) and (6.144) of [11] – with stator resistances neglected. This leaves us with $3n_g$ differential equations and $2n$ algebraic equations as functions of state variables δ_i , ω_i , and E'_{q_i} , for $i = 1 \dots n_g$, and algebraic variables θ_i and V_i , for $i = 1 \dots n$ as described below

$$\dot{\delta}_i = \omega_i - \omega_s \quad (1)$$

$$\frac{\dot{\omega}_i}{\omega_s} = \frac{T_{m_i}}{2H_i} - \frac{E'_{q_i} V_i \sin(\delta_i - \theta_i)}{2H_i x'_{d_i}} + \frac{V_i^2 \sin 2(\delta_i - \theta_i)}{4H_i} \left(\frac{x_{q_i} - x'_{d_i}}{x_{q_i} x'_{d_i}} \right) \quad (2)$$

$$\dot{E}'_{q_i} = \frac{E_{fd_i}}{T'_{do_i}} - \frac{E'_{q_i}}{T'_{do_i}} - \frac{E'_{q_i} - V_i \cos(\delta_i - \theta_i)}{x'_{d_i}} \left(\frac{x_{d_i} - x'_{d_i}}{T'_{do_i}} \right) \quad (3)$$

for $i = 1, \dots, n_g$

$$0 = f_i = \begin{cases} \frac{E'_{q_i} V_i \sin(\delta_i - \theta_i)}{x'_{d_i}} - \frac{V_i^2 \sin 2(\delta_i - \theta_i)}{2} \left(\frac{x_{q_i} - x'_{d_i}}{x_{q_i} x'_{d_i}} \right) \\ \quad + P_{L_i} - \sum_{k=1, k \neq i}^n V_i V_k Y_{ik} \sin(\theta_i - \theta_k) \\ \quad \text{for } i = 1, \dots, n_g \\ P_{L_i} - \sum_{k=1, k \neq i}^n V_i V_k Y_{ik} \sin(\theta_i - \theta_k) \\ \quad \text{for } i = n_g + 1, \dots, n \end{cases} \quad (4)$$

$$0 = g_i = \begin{cases} \frac{E'_{q_i} V_i \cos(\delta_i - \theta_i)}{x'_{d_i}} - \frac{V_i^2 \cos^2(\delta_i - \theta_i)}{x'_{d_i}} + Q_{L_i} - V_i^2 Y_{ii} \\ \quad - \frac{V_i^2 \sin^2(\delta_i - \theta_i)}{x_{q_i}} + \sum_{k=1, k \neq i}^n V_i V_k Y_{ik} \cos(\theta_i - \theta_k) \\ \quad \text{for } i = 1, \dots, n_g \\ Q_{L_i} + \sum_{k=1, k \neq i}^n V_i V_k Y_{ik} \cos(\theta_i - \theta_k) - V_i^2 Y_{ii} \\ \quad \text{for } i = n_g + 1, \dots, n \end{cases} \quad (5)$$

Linearizing (1) – (5) around an operating point, with V_{i_0} as the voltage magnitude of bus i at that point and defining a new variable $\nu_i = V_i/V_{i_0}$, we obtain

$$\begin{bmatrix} \Delta \dot{\delta} \\ \Delta \dot{\omega} \\ \Delta E'_{q_i} \end{bmatrix} = \mathbf{M} \begin{bmatrix} \Delta \delta \\ \Delta \omega \\ \Delta E'_{q_i} \end{bmatrix} + \mathbf{N} \begin{bmatrix} \Delta \theta \\ \Delta \nu \end{bmatrix} + \mathbf{B} \begin{bmatrix} \Delta T_m \\ \Delta E_{fd} \end{bmatrix} \quad (6)$$

$$\begin{bmatrix} \mathbf{0} \\ \mathbf{0} \end{bmatrix} = \mathbf{C} \begin{bmatrix} \Delta \delta \\ \Delta \omega \\ \Delta E'_{q_i} \end{bmatrix} + \mathbf{D} \begin{bmatrix} \Delta \theta \\ \Delta \nu \end{bmatrix}$$

where, δ , ω , E'_{q_i} , θ , and ν are the vectorized state and algebraic variables of respective type, for instance, $\delta = [\delta_i \dots \delta_{n_g}]^T$ and $\nu = [\nu_i \dots \nu_n]^T$. Finally, eliminating the algebraic variables, we get

$$\begin{bmatrix} \Delta \dot{\delta} \\ \Delta \dot{\omega} \\ \Delta E'_{q_i} \end{bmatrix} = \mathbf{A} \begin{bmatrix} \Delta \delta \\ \Delta \omega \\ \Delta E'_{q_i} \end{bmatrix} + \mathbf{B} \begin{bmatrix} \Delta T_m \\ \Delta E_{fd} \end{bmatrix} \quad (7)$$

where, $\mathbf{A} = \mathbf{M} - \mathbf{N}\mathbf{D}^{-1}\mathbf{C}$. It follows from the equations above that \mathbf{A} is of the form

$$\mathbf{A} = \begin{bmatrix} \mathbf{0} & \mathbf{I} & \mathbf{0} \\ \mathbf{A}_{21} & \mathbf{0} & \mathbf{A}_{23} \\ \mathbf{A}_{31} & \mathbf{0} & \mathbf{A}_{33} \end{bmatrix} \quad (8)$$

Note, in (8), every \mathbf{A}_{ij} block is a submatrix of \mathbf{A} whose elements are derived later in the paper (see, Appendix B). Apart from the state variables $\Delta \delta_i$, $\Delta \omega_i$, and $\Delta E'_{q_i}$, the output variable ΔT_{e_i} , which is the electromagnetic torque of generator i , is of specific interest to us. From the swing equation in (2) this is expressed as $\Delta T_{e_i} = -\frac{2H_i}{\omega_s} \Delta \dot{\omega}_i$.

Following any disturbance in the system or perturbation in the inputs, the time-evolution of these state and output variables can be expressed as sum of damped sinusoids with modal frequencies ω_{d_r} -s with differing amplitudes and phases. As a result, for each mode r , $\Delta T_{e_i,r}(t)$, $\Delta \delta_{i,r}(t)$ and $\Delta \omega_{i,r}(t)$ can be expressed as rotating phasors – for details, see Appendix A. The notions of damping torque and damping power for a given mode originate from the phasor representation of $\Delta \vec{T}_{e_i,r}$ in the $\Delta \vec{\delta}_{i,r} - \Delta \vec{\omega}_{i,r}$ plane and the power resulting from the interaction of the torque and the speed. This is explained next.

III. DAMPING POWER IN A MULTIMACHINE SYSTEM

In any i^{th} machine, for a mode r , let the average power of the electromagnetic torque $\Delta T_{e_{i,r}}(t)$ over a cycle starting from $t = t_0$ be denoted by $\dot{W}_{d_{i,r}}(t_0)$, as shown below

$$\dot{W}_{d_{i,r}}(t_0) = \frac{\int_{t_0}^{t_0 + \frac{2\pi}{\omega_{d_r}}} \Delta T_{e_{i,r}}(t) \Delta \omega_{i,r}(t) dt}{\int_{t_0}^{t_0 + \frac{2\pi}{\omega_{d_r}}} dt} \quad (9)$$

Using the phasor notation described in Appendix A, let $\Delta \vec{T}_{e_{i,r}}(t) = \beta_1 e^{\sigma_r t} \angle \gamma_1$ and $\Delta \vec{\omega}_{i,r}(t) = \beta_2 e^{\sigma_r t} \angle \gamma_2$. Therefore, $\dot{W}_{d_{i,r}}(t_0) =$

$$\begin{aligned} &= \frac{\omega_{d_r}}{2\pi} \int_{t_0}^{t_0 + \frac{2\pi}{\omega_{d_r}}} e^{2\sigma_r t} \beta_1 \cos(\omega_{d_r} t + \gamma_1) \beta_2 \cos(\omega_{d_r} t + \gamma_2) dt \\ &= \frac{\beta_1 \beta_2 \omega_{d_r}}{4\pi} \int_{t_0}^{t_0 + \frac{2\pi}{\omega_{d_r}}} e^{2\sigma_r t} \left\{ \cos(\gamma_1 - \gamma_2) \right. \\ &\quad \left. + \cos(2\omega_{d_r} t + \gamma_1 + \gamma_2) \right\} dt \\ &= \frac{\beta_1 \beta_2 \omega_{d_r}}{4\pi} \cos(\gamma_1 - \gamma_2) \frac{e^{2\sigma_r t_0}}{2\sigma_r} \left\{ e^{\frac{4\pi\sigma_r}{\omega_{d_r}}} - 1 \right\} \\ &\quad + \frac{\beta_1 \beta_2 \omega_{d_r}}{4\pi} \int_{t_0}^{t_0 + \frac{2\pi}{\omega_{d_r}}} e^{2\sigma_r t} \cos(2\omega_{d_r} t + \gamma_1 + \gamma_2) dt \end{aligned} \quad (10)$$

Now, considering that our mode of interest is poorly-damped (as is the premise of our paper), implying $|\sigma_r| \ll \omega_{d_r}$, we may expand the exponential $e^{\frac{4\pi\sigma_r}{\omega_{d_r}}}$ and neglect the second and higher order terms. On doing so, the first term in (10) reduces to

$$\begin{aligned} &\frac{\beta_1 \beta_2 \omega_{d_r}}{4\pi} e^{2\sigma_r t_0} \cos(\gamma_1 - \gamma_2) \frac{1 + \frac{4\pi\sigma_r}{\omega_{d_r}} - 1}{2\sigma_r} \\ &= \frac{1}{2} \beta_1 \beta_2 e^{2\sigma_r t_0} \cos(\gamma_1 - \gamma_2) \end{aligned}$$

With the same assumption that σ_r is small, the second term in (10) becomes negligible, and can be ignored for mathematical tractability. This is because, with $|\sigma_r| \ll \omega_{d_r}$, for a complete cycle of $\cos(2\omega_{d_r} t)$, the $e^{2\sigma_r t}$ term remains almost constant, and therefore, the positive and negative half cycles almost add to zero. Therefore,

$$\begin{aligned} \dot{W}_{d_{i,r}}(t_0) &\approx \frac{1}{2} \beta_1 \beta_2 e^{2\sigma_r t_0} \cos(\gamma_1 - \gamma_2) \\ &= \frac{1}{2} \Re \left\{ \beta_1 e^{\sigma_r t_0} \angle \gamma_1 \beta_2 e^{\sigma_r t_0} \angle -\gamma_2 \right\} \quad (11) \\ &= \frac{1}{2} \Re \left\{ \Delta \vec{T}_{e_{i,r}}(t_0) \Delta \vec{\omega}_{i,r}^*(t_0) \right\}. \end{aligned}$$

Hereafter, in the paper, assuming all phasors are computed at $t = t_0$ and powers are averaged over a cycle starting at t_0 , we shall drop the argument t_0 from our expressions.

From (11) it can be interpreted that $\dot{W}_{d_{i,r}}$ is the average power due to the component of $\Delta \vec{T}_{e_{i,r}}$ in the direction of $\Delta \vec{\omega}_{i,r}$. Let, the electromagnetic torque be decomposed as $\Delta \vec{T}_{e_{i,r}} = k_{d_{i,r}} \Delta \vec{\omega}_{i,r} + k_{s_{i,r}} (j \Delta \vec{\omega}_{i,r})$. Substituting this in (11), we get

$$\dot{W}_{d_{i,r}} = \frac{1}{2} \Re \left\{ (k_{d_{i,r}} + j k_{s_{i,r}}) \Delta \vec{\omega}_{i,r} \Delta \vec{\omega}_{i,r}^* \right\} = \frac{1}{2} k_{d_{i,r}} |\Delta \vec{\omega}_{i,r}|^2 \quad (12)$$

where, $k_{d_{i,r}} = \Re \left\{ \frac{\Delta \vec{T}_{e_{i,r}}}{\Delta \vec{\omega}_{i,r}} \right\}$ is the damping torque coefficient of machine i for mode r . Therefore, we shall refer to $\dot{W}_{d_{i,r}}$

as the ‘average damping power’ (or simply ‘damping power’) of $\Delta T_{e_{i,r}}(t)$. For a system with n_g machines, (11) can be extended as follows

$$\dot{W}_{d_r} = \sum_{i=1}^{n_g} \dot{W}_{d_{i,r}} = \frac{1}{2} \sum_{i=1}^{n_g} \Re \left\{ \Delta \vec{T}_{e_{i,r}} \Delta \vec{\omega}_{i,r}^* \right\} \quad (13)$$

Next, we express this sum of damping powers in terms of system matrices by using the definition of electromagnetic torque (from the swing equation) and the linearized system description obtained in (7) and (8), as shown below.

$$\begin{aligned} \Delta T_e(s) &= -\frac{2\mathbf{H}}{\omega_s} \Delta \dot{\omega}(s) = -\frac{2\mathbf{H}}{\omega_s} \left\{ \mathbf{A}_{21} \Delta \delta(s) + \mathbf{A}_{23} \Delta \mathbf{E}'_q(s) \right\} \\ &= -\frac{2\mathbf{H}}{\omega_s} \left\{ \mathbf{A}_{21} + \mathbf{A}_{23} (s\mathbf{I} - \mathbf{A}_{33})^{-1} \mathbf{A}_{31} \right\} \frac{\Delta \omega(s)}{s} \\ &\triangleq \mathbf{K}(s) \Delta \omega(s) \end{aligned} \quad (14)$$

Defining $\mathbf{K}_r = \mathbf{K}(j\omega_{d_r})$, we may re-write (13) as

$$\dot{W}_{d_r} = \frac{1}{2} \Re \left\{ \sum_{i=1}^{n_g} \sum_{j=1}^{n_g} \mathbf{K}_{ij,r} \Delta \vec{\omega}_{j,r} \Delta \vec{\omega}_{i,r}^* \right\} = \frac{1}{2} \Re \left\{ \Delta \vec{\omega}_r^H \mathbf{K}_r \Delta \vec{\omega}_r \right\} \quad (15)$$

where, $\mathbf{K}_{ij,r}$ is the $(i, j)^{\text{th}}$ element of \mathbf{K}_r . We call \dot{W}_{d_r} the ‘total damping power’ of the system for mode r .

Next, we simplify the expression in eqn (15) using the set of claims (1) – (4) below. Claims:

- (1) $\mathbf{P}^{-1} \mathbf{A}_{33}^T \mathbf{P} = \mathbf{A}_{33}$,
- (2) $\mathbf{A}_{31}^T \mathbf{P} = \frac{2\mathbf{H}}{\omega_s} \mathbf{A}_{23}$,
- (3) $2\mathbf{A}_{21}^T \mathbf{H} = 2\mathbf{H} \mathbf{A}_{21}$
- (4) $\forall \mathbf{x} \in \mathbb{C}^{n_g}, \Re \{ \mathbf{x}^H \mathbf{K}_r \mathbf{x} \} = \mathbf{x}^H \Re \{ \mathbf{K}_r \} \mathbf{x}$

where, \mathbf{P} is a diagonal matrix of machine parameters with $\mathbf{P}(i, i) = \frac{T_{d_{oi}}}{x_{d_i} - x'_{d_i}}$. Claims (1) – (3) are derived using the differential and algebraic equations of the system modeled in Section II. These claims are then used to establish the symmetry of \mathbf{K}_r , which is in-turn used in proving claim (4). Detailed proof of these claims are outlined in Appendix B.

Using claim (4) we further reduce eqn (15) as follows

$$\dot{W}_{d_r} = \frac{1}{2} \Delta \vec{\omega}_r^H \Re \{ \mathbf{K}_r \} \Delta \vec{\omega}_r \quad (16)$$

where, $\Re \{ \mathbf{K}_r \} =$

$$\begin{aligned} &= -\Re \left\{ \frac{2\mathbf{H}}{j\omega_{d_r} \omega_s} \left(\mathbf{A}_{21} + \mathbf{A}_{23} (j\omega_{d_r} \mathbf{I} - \mathbf{A}_{33})^{-1} \mathbf{A}_{31} \right) \right\} \\ &= -\frac{2\mathbf{H}}{\omega_s} \mathbf{A}_{23} \Re \left\{ (-j\omega_{d_r} \mathbf{I} - \mathbf{A}_{33}) (-j\omega_{d_r} \mathbf{I} - \mathbf{A}_{33})^{-1} \right. \\ &\quad \left. \frac{(j\omega_{d_r} \mathbf{I} - \mathbf{A}_{33})^{-1}}{j\omega_{d_r}} \right\} \mathbf{A}_{31} \\ &= -\frac{2\mathbf{H}}{\omega_s} \mathbf{A}_{23} \Re \left\{ \frac{(-j\omega_{d_r} \mathbf{I} - \mathbf{A}_{33}) (\omega_{d_r}^2 \mathbf{I} + \mathbf{A}_{33}^2)^{-1}}{j\omega_{d_r}} \right\} \mathbf{A}_{31} \\ &= \frac{2\mathbf{H}}{\omega_s} \mathbf{A}_{23} (\omega_{d_r}^2 \mathbf{I} + \mathbf{A}_{33}^2)^{-1} \mathbf{A}_{31} \end{aligned}$$

This, along with claim (2) when substituted in eqn (16) gives

$$\dot{W}_{d_r} = \frac{1}{2} \Delta \vec{\omega}_r^H \mathbf{A}_{31}^T \mathbf{P} (\omega_{d_r}^2 \mathbf{I} + \mathbf{A}_{33}^2)^{-1} \mathbf{A}_{31} \Delta \vec{\omega}_r \quad (17)$$

IV. CONSISTENCY OF DAMPING POWER WITH POWER DISSIPATION IN SYNCHRONOUS MACHINE WINDINGS

Considering the third-order system model in Section II, the only source of power dissipation in the machines is in the field windings. For any mode r , we denote the average power dissipation in the winding of machine i by $\dot{W}_{f_{i,r}}$. Following the phasor notation as discussed, this is expressed as

$$\begin{aligned}\dot{W}_{f_{i,r}} &= \frac{1}{2} \Re \left\{ (\Delta \vec{I}_{f_{i,r}} R_{f_i}) \Delta \vec{I}_{f_{i,r}}^* \right\} = \frac{1}{2} R_{f_i} \left| \Delta \vec{I}_{f_{i,r}} \right|^2 \\ &= \frac{1}{2} \frac{T'_{do_i}}{x_{d_i} - x'_{d_i}} \left| \Delta \vec{E}'_{q_{i,r}} \right|^2\end{aligned}\quad (18)$$

where, $\Delta \vec{I}_{f_{i,r}}$ and $\Delta \vec{E}'_{q_{i,r}}$ are the phasors of the field current and derivative of transient e.m.f. due to field flux linkage, respectively. Further, using notations from (36) (Appendix A) we may write

$$\Delta \vec{E}'_{q_{i,r}} = j\omega_{d_r} \Delta \vec{E}'_{q_{i,r}} = j\omega_{d_r} 2 c_r e^{\sigma_r t_0} \psi_{E'_{q_{i,r}}}. \quad (19)$$

We define, $\hat{c}_r = c_r e^{\sigma_r t_0}$. Next, substituting (19) in (18) we get

$$\dot{W}_{f_{i,r}} = 2 |\hat{c}_r|^2 \frac{T'_{do_i}}{x_{d_i} - x'_{d_i}} \omega_{d_r}^2 \left| \psi_{E'_{q_{i,r}}} \right|^2. \quad (20)$$

We obtain the total power dissipation for the mode by adding the dissipation in individual machines. This is shown below.

$$\dot{W}_{f_r} = \sum_{i=1}^{n_g} \dot{W}_{f_{i,r}} = 2 |\hat{c}_r|^2 \omega_{d_r}^2 \Psi_{E'_{q_r}}^H \mathbf{P} \Psi_{E'_{q_r}} \quad (21)$$

where, $\Psi_{E'_{q_r}} = \begin{bmatrix} \psi_{E'_{q_{1,r}}} & \cdots & \psi_{E'_{q_{i,r}}} & \cdots & \psi_{E'_{q_{n_g,r}}} \end{bmatrix}^T$.

To show that our notion of total damping power, as defined in Section III, is consistent with the power dissipated in the system, we need to prove that for any mode r , \dot{W}_{f_r} is equal to \dot{W}_{d_r} . To do so, we make the following algebraic manipulations.

First, since λ_r is an eigenvalue of the system, we may write $\mathbf{A}\Psi_r = \lambda_r\Psi_r$, where, the right eigenvector $\Psi_r = \begin{bmatrix} \Psi_{\delta_r} & \Psi_{\omega_r} & \Psi_{E'_{q_r}} \end{bmatrix}^T$. Next, using the structure of matrix \mathbf{A} as in (8), we can split this into the following equations

$$\Psi_{E'_{q_r}} = (\lambda_r \mathbf{I} - \mathbf{A}_{33})^{-1} \mathbf{A}_{31} \Psi_{\delta_r} \quad \text{and} \quad \Psi_{\delta_r} = \frac{1}{\lambda_r} \Psi_{\omega_r}. \quad (22)$$

Using these, along with (34) describing $\Delta \vec{\omega}_r = 2 \hat{c}_r \Psi_{\omega_r}$, we may re-write (21) as follows

$$\begin{aligned}\dot{W}_{f_r} &= 2 |\hat{c}_r|^2 \omega_{d_r}^2 \frac{\Delta \vec{\omega}_r^H}{2 c_r^* \lambda_r^*} \mathbf{A}_{31}^T (\lambda_r^* \mathbf{I} - \mathbf{A}_{33}^T)^{-1} \mathbf{P} \\ &\quad (\lambda_r \mathbf{I} - \mathbf{A}_{33})^{-1} \mathbf{A}_{31} \frac{\Delta \vec{\omega}_r}{2 c_r \lambda_r}.\end{aligned}\quad (23)$$

Finally, considering that our mode of interest is poorly-damped $|\sigma_r| \ll \omega_{d_r}$ – as is the premise of [14], and for consistency this paper's too, we substitute $\lambda_r = j\omega_{d_r}$ in (23). This, along with use of claim (1) reduces (23) as follows

$$\begin{aligned}\dot{W}_{f_r} &= \frac{1}{2} \Delta \vec{\omega}_r^H \mathbf{A}_{31}^T (-j\omega_{d_r} \mathbf{I} - \mathbf{P} \mathbf{A}_{33} \mathbf{P}^{-1})^{-1} \mathbf{P} \\ &\quad (j\omega_{d_r} \mathbf{I} - \mathbf{A}_{33})^{-1} \mathbf{A}_{31} \Delta \vec{\omega}_r \\ &= \frac{1}{2} \Delta \vec{\omega}_r^H \mathbf{A}_{31}^T \mathbf{P} (\omega_{d_r}^2 \mathbf{I} + \mathbf{A}_{33}^2)^{-1} \mathbf{A}_{31} \Delta \vec{\omega}_r = \dot{W}_{d_r}.\end{aligned}\quad (24)$$

Thus, for any given mode, the equivalence of the total damping power and the sum of average rate of change of energy dissipations in the machine windings is established.

Remarks: (1) While the concepts of damping torque and damping power are derived using the linearized system models, the average rate of energy dissipation in windings are more fundamental and does not limit itself to small-signal analysis.

(2) For machines with detailed models, the power dissipation in damper windings should be added to \dot{W}_{f_r} to obtain the total dissipation in the system. Average power dissipation in the damper winding is expressed as [13]

$$\dot{W}_{g_{i,r}} = 2 |\hat{c}_r|^2 \frac{T'_{do_i}}{x_{q_i} - x'_{q_i}} \omega_{d_r}^2 \left| \psi_{E'_{d_{i,r}}} \right|^2. \quad (25)$$

$E'_{d_{i,r}}$ is the state variable describing the dynamics of the damper winding transient e.m.f. Further, with dynamics of the excitation systems modeled, the expression of \dot{W}_{f_r} in (21) would get modified to include the effect of $\Delta \mathbf{E}_{fd}$ as

$$\begin{aligned}\dot{W}_{f_{i,r}} &= 2 |\hat{c}_r|^2 \left\{ \frac{T'_{do_i}}{x_{d_i} - x'_{d_i}} \omega_{d_r}^2 \left| \psi_{E'_{q_{i,r}}} \right|^2 \right. \\ &\quad \left. - \frac{1}{x_{d_i} - x'_{d_i}} \Re \left(j\omega_{d_r} \psi_{E'_{q_{i,r}}} \psi_{E'_{fd_{i,r}}}^* \right) \right\}.\end{aligned}\quad (26)$$

However, the expression for \dot{W}_{d_r} in (15) would remain the same (with block matrices \mathbf{A}_{23} , \mathbf{A}_{31} , and \mathbf{A}_{33} larger in dimensions to account for the additional state variables like $\Delta \mathbf{E}'_d$, $\Delta \mathbf{E}_{fd}$, etc. now concatenated to the vector $\Delta \mathbf{E}'_q$) and the equality of total damping power and total power dissipation would still be true. This will be demonstrated in Section VI.

(3) Additionally, with a power system stabilizer (PSS) and an IEEE ST1A exciter modeled, as shown in Fig. 1, three new states will be added – one each due to the washout block, the lead-lag compensator, and the time constant of the transducer. Concatenating these to the existing state variables, the block matrices \mathbf{A}_{23} , \mathbf{A}_{31} , and \mathbf{A}_{33} would be further expanded. Additionally, due to the speed feedback to the washout block, \mathbf{A}_{32} term would now be non-zero, implying,

$$\mathbf{K}_r = \frac{2 \mathbf{H}}{\omega_s} \left(\frac{\mathbf{A}_{21}}{j\omega_{d_r}} + \mathbf{A}_{23} (j\omega_{d_r} \mathbf{I} - \mathbf{A}_{33})^{-1} \left(\frac{\mathbf{A}_{31}}{j\omega_{d_r}} + \mathbf{A}_{32} \right) \right).$$

The equality of total damping power \dot{W}_{d_r} (as calculated with the modified \mathbf{K}_r) and that of the sum of \dot{W}_{f_r} and \dot{W}_{g_r} will be demonstrated in Section VI.

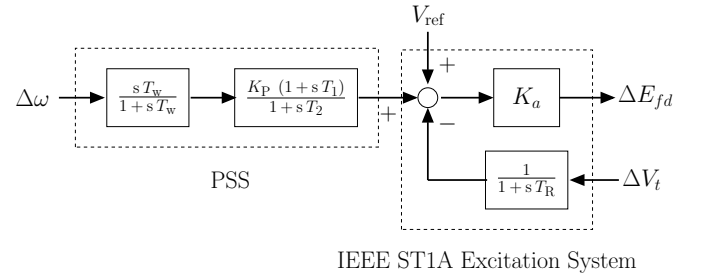


Fig. 1: PSS and IEEE ST1A excitation system.

(4) Next, let us explore the importance of our deductions in the context of stability monitoring. From [13], we know that, the relative damping contribution of individual generators can be inferred from the power dissipations in their windings.

Further, our paper establishes $\sum \dot{W}_{d_{i,r}} = \sum (\dot{W}_{f_{i,r}} + \dot{W}_{g_{i,r}})$, which building on derivations in [13] leads to the claim that the stability margin of the r^{th} mode $\sigma_r \propto -\sum \dot{W}_{d_{i,r}}$. Note that, estimating the variables ΔT_{e_i} and $\Delta \omega_i$ are relatively simpler. Because, either they can be directly measured, as with rotor speed, or estimated from measurable outputs, like torque from power. And therefore, damping power $\dot{W}_{d_{i,r}}$ of individual machines can be easily calculated from their terminal measurements upon filtering for the mode of interest. This has the potential for future monitoring applications, like determining stability margin of a mode by measuring total damping power contribution from all generators. To this end, it is important to clarify that, we do not claim efficacy over the existing mode-metering algorithms like [16] (which would anyways be required to identify the poorly-damped modes in the system), instead, we propose $\sum \dot{W}_{d_{i,r}}$ as a complementary measure of stability margin for the mode, with individual $\dot{W}_{d_{i,r}}$ -s as indices for identifying the prospective generator locations for damping enhancement.

V. DISTRIBUTION FACTORS: EXPRESSING DAMPING POWER OF EACH MACHINE AS WEIGHTED SUM OF DISSIPATIONS IN ALL MACHINES

With the equality in (24) now proved, it might be tempting to draw an intuitive conclusion that such a power balance should hold for individual generators. However, this is not the case. This is because, the modeshape of E'_q of each generator is a function of modeshapes of speed-deviation of all other machines and vice-versa (see, (22)). Therefore, the mathematical representation of damping power in each machine is in reality an abstraction of dissipative effects coming from the windings of all machines in the system including it's own. To that end, we next derive the distribution factors describing the fractional contribution of windings of different machines in constituting the damping power of a single machine.

Considering the system model described in Section II, in this section, we express the damping power of each generator $\dot{W}_{d_{i,r}}$ as a linear combination of individual $\dot{W}_{f_{i,r}}$ -s. Recall, from (12)

$$\dot{W}_{d_{i,r}} = \frac{1}{2} k_{d_{i,r}} \left| \Delta \vec{\omega}_{i,r} \right|^2 = 2 |\hat{c}_r|^2 k_{d_{i,r}} \Psi_{\omega_r}^H \mathbf{I}_i \Psi_{\omega_r} \quad (27)$$

where, \mathbf{I}_i is a n_g -dimensional square matrix with the $(i, i)^{th}$ entry as 1 and remaining all entries as zeros. Next, from the eigen decomposition of \mathbf{A} as before, we may write $\Psi_{\omega_r} = \lambda_r (\lambda_r^2 \mathbf{I} - \mathbf{A}_{21})^{-1} \mathbf{A}_{23} \triangleq \mathbf{Q} \Psi_{E'_{qr}}$. Substituting this, (27) may be expressed as

$$\begin{aligned} \dot{W}_{d_{i,r}} &= 2 |\hat{c}_r|^2 k_{d_{i,r}} \Psi_{E'_{qr}}^H \mathbf{Q}^H \mathbf{I}_i \mathbf{Q} \Psi_{E'_{qr}} \\ &= 2 |\hat{c}_r|^2 k_{d_{i,r}} \sum_{\ell=1}^{n_g} \sum_{j=1}^{n_g} Q_{i\ell}^* Q_{ij} \psi_{E'_{q\ell,r}}^* \psi_{E'_{qj,r}} \\ &= \sum_{j=1}^{n_g} 2 |\hat{c}_r|^2 k_{d_{i,r}} \frac{Q_{ij} \sum_{\ell=1}^{n_g} Q_{i\ell}^* \psi_{E'_{q\ell,r}}^*}{\psi_{E'_{qj,r}}^*} \left| \psi_{E'_{qj,r}} \right|^2 \\ &= \sum_{j=1}^{n_g} \frac{k_{d_{i,r}}}{P_j \omega_{d_r}^2} \frac{Q_{ij} \psi_{\omega_{i,r}}^*}{\psi_{E'_{qj,r}}^*} \dot{W}_{f_{j,r}} \end{aligned} \quad (28)$$

where, P_j is the diagonal element $\mathbf{P}(j, j) = \frac{T'_{d_{oj}}}{x_{d_j} - x'_{d_j}}$. Next, we define β_{ij} as the component of $\Delta \vec{\omega}_{i,r}$ due to $\Delta E'_{qj,r}$

$$\beta_{ij} \triangleq \left(\frac{Q_{ij} \Delta \vec{E}'_{qj,r}}{\Delta \vec{\omega}_{i,r}} \right)^* = \frac{Q_{ij}^* \psi_{E'_{qj,r}}^*}{\psi_{\omega_{i,r}}^*}. \quad (29)$$

Since, $\psi_{\omega_{i,r}}^* = \sum_{j=1}^{n_g} Q_{ij}^* \psi_{E'_{qj,r}}^*$, we may say $Q_{ij}^* \psi_{E'_{qj,r}}^*$ is the contribution of $\psi_{E'_{qj,r}}^*$ in the modeshape $\psi_{\omega_{i,r}}^*$. Therefore,

$$\dot{W}_{d_{i,r}} = \sum_{j=1}^{n_g} \frac{k_{d_{i,r}} |Q_{ij}|^2}{P_j \omega_{d_r}^2 \beta_{ij}} \dot{W}_{f_{j,r}} \quad (30)$$

Since, $\dot{W}_{d_{i,r}}$ -s and $\dot{W}_{f_{i,r}}$ -s are real quantities, the imaginary part of (30) is zero. Hence,

$$\dot{W}_{d_{i,r}} = \sum_{j=1}^{n_g} \frac{k_{d_{i,r}} |Q_{ij}|^2}{P_j \omega_{d_r}^2} \Re \left(\frac{1}{\beta_{ij}} \right) \dot{W}_{f_{j,r}} \triangleq \sum_{j=1}^{n_g} \alpha_{ij} \dot{W}_{f_{j,r}} \quad (31)$$

We call α_{ij} -s the ‘distribution factors,’ because, for a fixed i , the ratios $\alpha_{ij} \frac{\dot{W}_{f_{j,r}}}{\dot{W}_{d_{i,r}}}$ for $j = 1$ to n_g , are the fractions in which the damping power of generator i is derived from the power dissipation in the windings of the machines 1 to n_g . Further, looking from the other side, fixing a machine j , the factors α_{ij} -s describe the ratios in which the power dissipation in that machine winding is *distributed* in the ‘abstract’ damping power of all other machines.

A. Connection to the Heffron-Phillips Model

We know from the Heffron-Phillips model [17] of a SMIB system that, for a third-order machine model ($K1 - K4$ model), the angle between the $\Delta \vec{T}_{e_{i,r}}$ and $\Delta \vec{\omega}_{i,r}$ phasors is determined by the field circuit time-constant. Higher the resistance of the field circuit, smaller is the angle, and therefore, higher is the damping power of the generator. This is consistent with the results in [14] that for a SMIB system, the damping power of the machine is derived exclusively from the power dissipation in its field circuit. Extending the same to the Heffron-Phillips model for multimachine systems, we see (from Fig. 6 in [18]) that the damping power of each generator has contributions from the field circuit dissipations in multiple other machines in the system – depending on the relative participation of those machines in the mode of interest. However, given the complexity in calculating the modewise $K1 - K4$ constants in a multimachine system, we, through the distribution factors derived in this section, offer an alternative path to express the damping powers of each generator as a weighted sum of field winding dissipations of all machines in the system, including it's own.

B. Potential Application in Understanding Dissipative Contribution from PSS and Other Controllers

The lead-lag compensators in a $\Delta\omega$ -PSS are designed knowing the angular relationship between the $\Delta \vec{T}_{e_{i,r}}$ and $\Delta \vec{\omega}_{i,r}$ phasors, and the phase-shift required to rotate $\Delta \vec{T}_{e_{i,r}}$ further in the direction of $\Delta \vec{\omega}_{i,r}$. This phase-shift introduces additional damping for the mode by increasing the total power loss in the system for the mode for which the PSS is designed. However, since a PSS in one location might negatively affect

the damping in some other location, dissipation in some individual generators may be reduced. While, methods like the one in [18] quantify the effect of PSS on damping powers of individual machines, they do not describe how the dissipations in their windings would change. To this end, the distribution factors connecting damping and dissipative powers become useful. Also, this is not limited to PSSs in generators, if derived for higher-order models, the analysis can be extended to other types of controllers.

While distribution factors may not have direct usefulness in terms of monitoring or controlling a mode, we believe they serve as an important tool that bridge an insightful link between two apparently different frameworks.

VI. CASE STUDIES

We now verify the aforementioned claims on the fundamental frequency phasor models of IEEE 4-machine [17] and 16-machine [19] test systems. In each case we consider two types of models: (a) *Simplified model* with assumptions described in Section II, and (b) *Detailed model* considering 4th-order synchronous machine dynamics (including 1 damper winding) along with exciters, where the network is still assumed to be lossless and loads are of constant power nature.

A. IEEE 2–area 4–machine Kundur Test System

Consider the 4–machine system [17] shown in Fig. 2 with a total load of 2,734 MW under nominal condition.

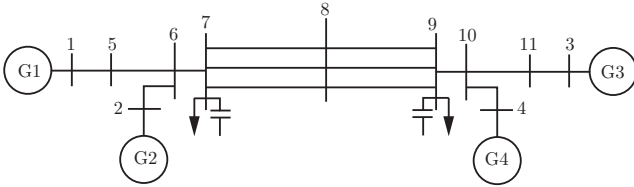


Fig. 2: Single-line diagram of 2–area 4–machine test system.

(a) *Simplified model*: Under nominal loading, there are three poorly-damped modes, see Table I. Given modeling assumptions, the only source of damping is in the field windings of the generators. Therefore, following our proposition, we need to show that for small perturbations in the system, for each of these oscillatory modes, the sum of average damping powers is numerically equal to the sum of power dissipations in the field windings, across the operating points. This is demonstrated in the Figs. 3 (a) and (b) for two of the three modes. The operating point is varied by progressively reducing the tie flow between buses 7 and 9 from 433 MW under nominal condition to -400 MW while maintaining the total load of the system constant.

We now validate our claim that although the total power dissipation is equal to the total damping power at the system level, this is not necessarily true for individual machines. In Figs 4 (a) and (b), the ratios of dissipation power to damping power is plotted for each of the 4 machines for the 0.69 Hz and 1.04 Hz modes, respectively. Observe that the ratios show strict monotonicity with change in operating points and under no circumstance they are equal to 1 all at once.

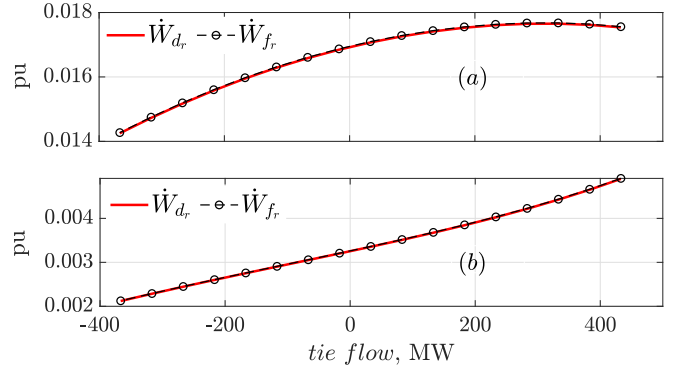


Fig. 3: Equality of total damping power with sum of average power dissipation in field windings of all generators across different operating points in simplified 4–machine system model for (a) 0.69 Hz and (b) 1.04 Hz modes.

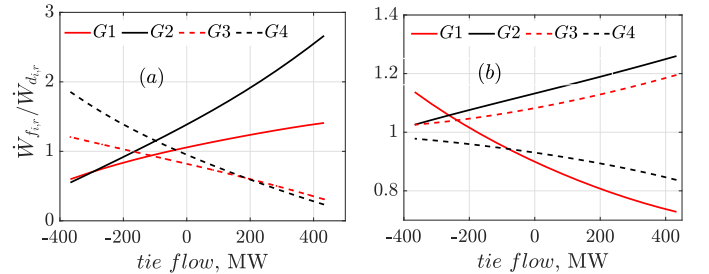


Fig. 4: Ratios of average power dissipation in field windings ($\dot{W}_{f,r}$) and that due to damping torques ($\dot{W}_{d,r}$) for individual machines across different operating points in simplified 4–machine system model for (a) 0.69 Hz and (b) 1.04 Hz modes.

Next, in Fig. 5, the relative contributions from the power dissipations in the windings of G1 to G4 in constituting the damping power of G1, as discussed in Section V, are plotted for the 0.69 Hz mode. Observe that, at a given operating point, the fractions $\alpha_{1j} \frac{\dot{W}_{f,j,r}}{\dot{W}_{d1,r}}$ for $j = 1$ to 4 add to 1. In Fig. 6 the distribution factors α_{i1} -s for $i = 1$ to 4 are shown. These describe fractions in which the power of oscillatory energy dissipation in G1 is distributed in the damping powers of G1 to G4. It can be seen that at any operating point, $\sum_{i=1}^4 \alpha_{i1} = 1$. Since the machines are nearly identical and the network is symmetric with respect to the generators in this system, the nature of the distribution factors are similar for other generators, and thus are not repeated here.

(b) *Detailed model*: The detailed model considers DC1A excitation system [17] for each generator over and above the

TABLE I: POORLY-DAMPED MODES IN IEEE 4-MACHINE SYSTEM

Machine Model	Eigenvalues $\lambda_r = \sigma_r \pm j\omega_{d_r}$	Modal freq. f_r (Hz)	Damp. ratio ζ_r
Simplified model	$-0.1183 \pm j4.3816$	0.69	0.027
	$-0.1444 \pm j6.2779$	1.00	0.023
	$-0.1544 \pm j6.5330$	1.04	0.024
Detailed model (with DC1A exciters)	$-0.1231 \pm j4.2130$	0.67	0.029
Detailed model (with ST1A exciters & PSS)	$-0.1477 \pm j4.8649$	0.77	0.030

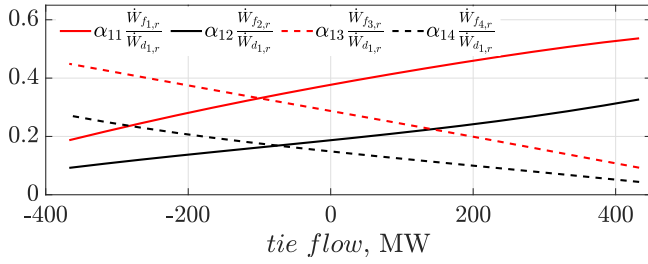


Fig. 5: Fractions in which the damping power of G1 is distributed as power dissipation in the windings of G1 – G4 for 0.69 Hz mode.

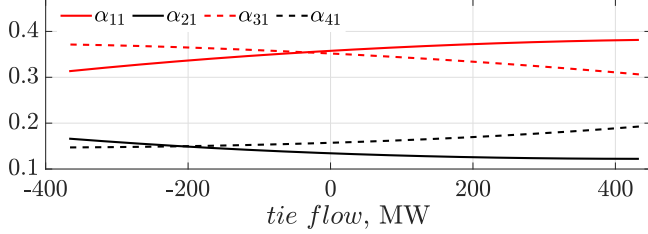


Fig. 6: Distribution of the power dissipation in G1 in the damping powers of G1 – G4 for 0.69 Hz mode.

assumptions mentioned earlier – the poorly-damped mode is shown in Table I. For any mode, the power dissipation in the system is the summation of total power dissipations in field winding \dot{W}_{f_r} and in damper winding \dot{W}_{g_r} (see, (26) and (25), respectively), where $\dot{W}_{f_r} = \sum_{i=1}^{n_g} \dot{W}_{f_{i,r}}$ and $\dot{W}_{g_r} = \sum_{i=1}^{n_g} \dot{W}_{g_{i,r}}$. For the detailed model, the consistency of total power dissipation with the total damping power is illustrated in Fig. 7.

(c) *Validation under large disturbances:* Next, we consider the 4th-order machine model with IEEE ST1A excitation system for validation under large disturbances. Additionally, G1 is equipped with a PSS. We simulate a 5-cycle three-phase self-clearing fault at $t = 1$ s near bus 8. The detrended post-fault time-domain plots of the state and output variables of the two generators G1 and G3 are shown in Fig. 8. We obtain the relative modeshapes of these signals using the approach described in [20].

We use $\Delta\omega_1$ as the reference signal and compute the modeshapes for all $\Delta\omega_i$, ΔT_{e_i} , $\Delta E'_{q_i}$, $\Delta E'_{d_i}$, and $\Delta E_{f_{d_i}}$ -s for the critical mode in Table I. The damping and dissipative powers of all 4 generators as computed using these modeshapes are shown in Table II. It can be seen that, although for individual

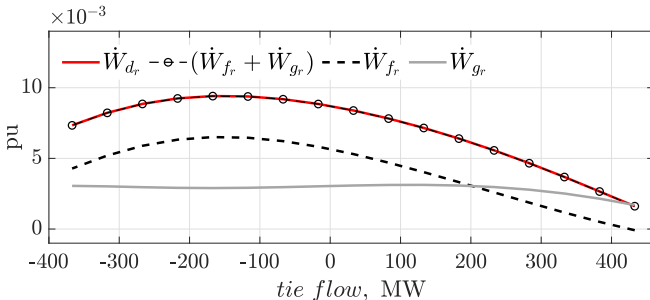


Fig. 7: Equality of total damping power with sum of average power dissipation in windings of all generators across different operating points in detailed 4-machine system model for the 0.67 Hz mode.

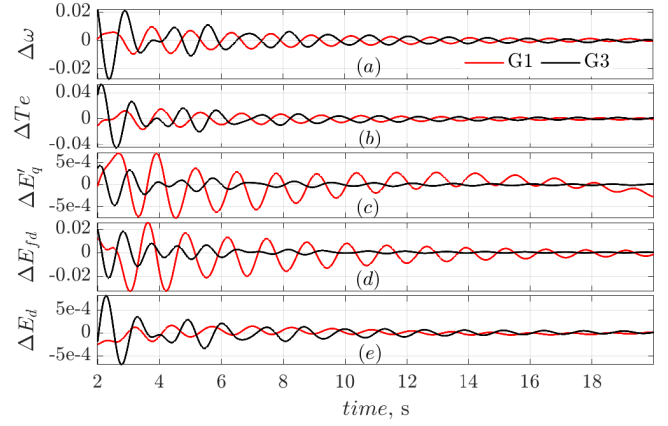


Fig. 8: Detrended post-fault time-domain plots of the state and output variables of G1 and G3.

TABLE II: DAMPING AND DISSIPATIVE POWERS IN DETAILED 4-MACHINE SYSTEM MODEL FOR 0.77 Hz MODE.

	Using the eigenvectors obtained from the small-signal model		Using the modeshapes estimated from the time-domain responses	
	$\frac{\dot{W}_{d_{i,r}}}{2 \hat{c}_r ^2}$	$\frac{\dot{W}_{f_{i,r}}}{2 \hat{c}_r ^2}$	$\frac{\dot{W}_{d_{i,r}}}{2 \hat{c}_r ^2}$	$\frac{\dot{W}_{f_{i,r}}}{2 \hat{c}_r ^2}$
G1	0.0382	0.2294	0.0361	0.2274
G2	0.0321	-0.1830	0.0340	-0.1877
G3	0.0435	0.0794	0.0405	0.0754
G4	0.0521	0.0401	0.0472	0.0390
Sum	0.1659	0.1659	0.1578	0.1541

machines the values of $\dot{W}_{d_{i,r}}$ -s are different from that of $\dot{W}_{f_{i,r}}$ -s, their sum totals are almost equal. Also, these values nearly match those calculated from the small-signal model.

TABLE III: POORLY-DAMPED MODES IN 16-MACHINE SYSTEM

Machine Model	Eigenvalue	Modal freq.	Damping ratio
	$\lambda_r = \sigma_r + j\omega_{d_r}$	f_r (Hz)	ζ_r
Simplified model	$-0.0336 \pm j2.1031$	0.34	0.016
	$-0.0338 \pm j3.1288$	0.50	0.011
	$-0.1062 \pm j3.7500$	0.60	0.028
	$-0.0264 \pm j4.1031$	0.65	0.006
Detailed model	$-0.0656 \pm j3.1137$	0.49	0.021
	$-0.0981 \pm j3.5169$	0.56	0.028
	$-0.1827 \pm j4.9627$	0.79	0.037

B. IEEE 5-area 16-machine NY-NE Test System

Next, consider the 16-machine New York-New England test system shown in Fig. 9. In the detailed model, G1 – G8 have DC1A exciters, G9 is equipped with a ST1A exciter and a power system stabilizer (PSS), and the remaining generators have manual excitation. The machine and the network data can be obtained from [19]. The poorly damped modes of the system under nominal loading, for both simplified and detailed models, are shown in Table. III. Different operating points are obtained by uniformly changing the total system load. As before, in Figs 10 and 11, the consistency of total damping power and sum of power dissipation in machine windings is

shown respectively for the simplified and the detailed model – each corresponding to a particular mode. The negative values of $\dot{W}_{f,r}$ in Fig.11 indicate that the excitation systems are contributing towards negative damping for higher loadings.

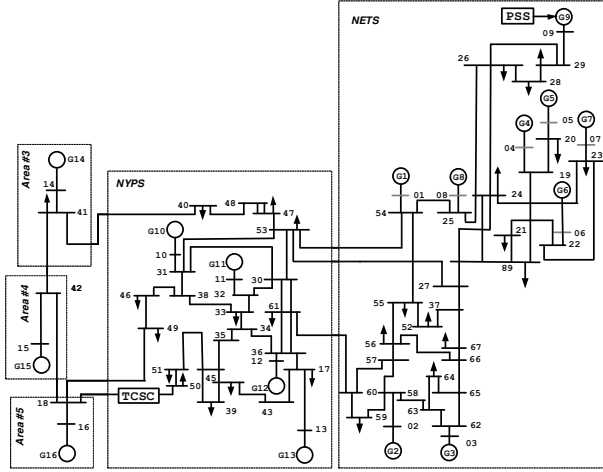


Fig. 9: Single-line diagram of IEEE 5–area 16–machine NY-NE test system.

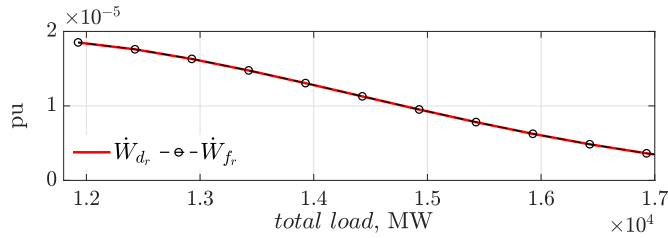


Fig. 10: Equality of total damping power with sum of average power dissipation in field windings of all generators across different operating points in simplified 16–machine system model for 0.50 Hz mode.

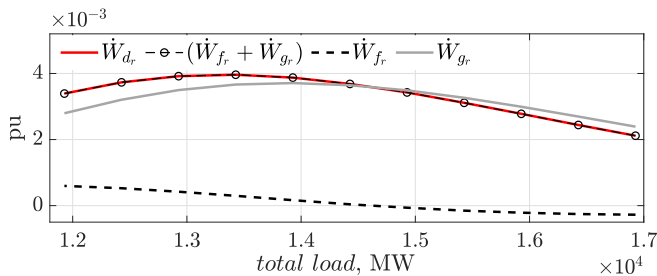


Fig. 11: Equality of total damping power with sum of average power dissipation in windings of all generators across different operating points in detailed 16–machine system model for 0.56 Hz mode.

Next, we present the following case study for the simplified model to validate our claims regarding the distribution of damping power. In this study, for G9, we compare the values of $\frac{\alpha_{9j} \dot{W}_{fj,r}}{\dot{W}_{d9,r}}$ (fractions in which the damping power of G9 is derived from the power dissipations in the windings of any j^{th} generator) as calculated from small-signal model and as estimated from time-domain responses. Under nominal loading condition, a 0.2 s pulse disturbance is applied to the excitation system of all generators and the time-domain responses of the state and output variables are obtained. Detrended plots of the variables of G9 are shown in Fig. 12. Using the approach in [20] as before, we next estimate the relative modeshapes

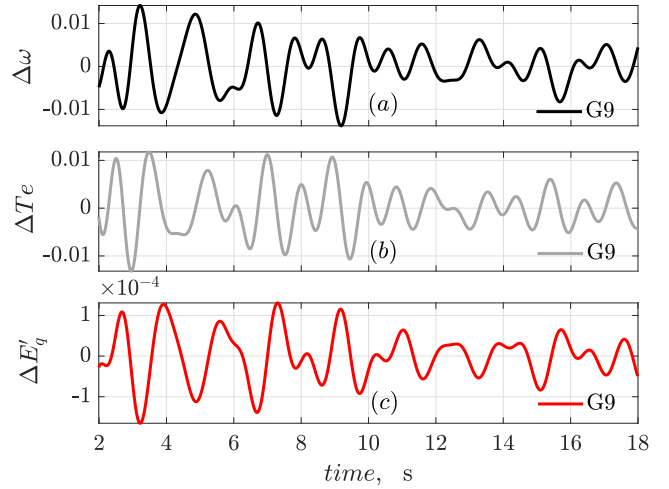


Fig. 12: Detrended time-domain responses of (a) ω , (b) T_e , and (c) E'_q of G9 following a pulse disturbance in the excitation system of all generators in the 16–machine system.

of ω_g , T_{e9} , and E'_{q9} , along with E'_{qi} for selected generators: G3, G5, and G6 from NETS, and G11 from NYPS from their time-domain responses. We use $\Delta\omega_g$ as the reference and the modeshapes are estimated for the 0.6 Hz mode. For this mode, the generators of NETS oscillate against those in NYPS. Next, using the estimated modeshapes, we compute the damping and dissipative powers of the selected generators as shown in Table IV. Finally, using the α_{ij} -s from the expression in (30) and the values estimated in Table IV, we compute the fractional contributions from these selected generators towards the damping power of G9. These are shown in Table V. As seen, the estimated values match those calculated from small-signal model. The variation in these fractions for change in system loading are shown in Fig. 13.

TABLE IV: DAMPING AND DISSIPATIVE POWERS FOR THE 0.6 Hz MODE ESTIMATED FROM TIME-DOMAIN RESPONSES

$\frac{\dot{W}_{d9,r}}{2 \hat{e}_r ^2}$	$\frac{\dot{W}_{f3,r}}{2 \hat{e}_r ^2}$	$\frac{\dot{W}_{f5,r}}{2 \hat{e}_r ^2}$	$\frac{\dot{W}_{f6,r}}{2 \hat{e}_r ^2}$	$\frac{\dot{W}_{f9,r}}{2 \hat{e}_r ^2}$	$\frac{\dot{W}_{f11,r}}{2 \hat{e}_r ^2}$
0.0806	0.0905	0.0663	0.0791	0.1340	0.0334

TABLE V: FRACTIONAL CONTRIBUTION FROM SELECTED GENERATORS TOWARDS DAMPING POWER OF G9 FOR THE 0.6 Hz MODE

frac. contr. from	G9	G3	G5	G6	G11
small-signal model	0.2064	0.1382	0.1063	0.1102	0.0520
time-domain estimation	0.2046	0.1369	0.1003	0.1198	0.0501

Now, we consider the other poorly-damped mode at 0.5 Hz, for which generators outside NETS – G14 and G16 oscillate against each other with marginal participation from generators in other areas. The damping and dissipative powers of these two generators, for the mode, are shown in Table VI. Note that, since other generators do not participate in the mode, the summation of damping powers of G14 and G16 is approximately equal to the summation of their dissipative powers. Finally, in Fig. 14, the relative dissipative contributions from the generators in different areas in constituting the damping

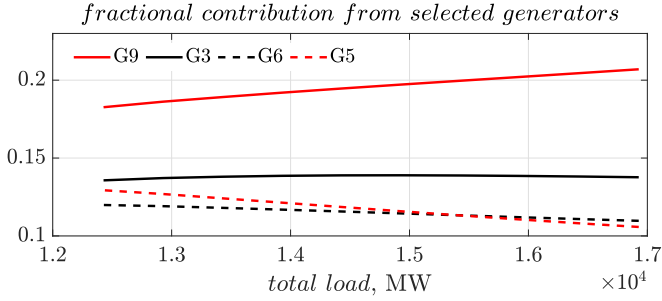


Fig. 13: Fractions in which the damping power of G9 is derived from the power dissipations in the windings of selected generators in NETS: G3, G5, G6, and G9 for the 0.60 Hz mode.

power of G16 are shown. For G1 – G9 and G10 – G13, their aggregates

$$\sum_{j=1}^9 \alpha_{16,j} \frac{\dot{W}_{f_{j,r}}}{\dot{W}_{d_{16,r}}} \quad \text{and} \quad \sum_{j=10}^{13} \alpha_{16,j} \frac{\dot{W}_{f_{j,r}}}{\dot{W}_{d_{16,r}}}$$

are shown as contributions from NETS and NYPS, respectively. We note that G14 and G16 have the highest participation in the mode, which is aligned with the observation that these generators have the highest dissipative contribution.

TABLE VI: DAMPING AND DISSIPATIVE POWERS OF G14 and G16 FOR THE 0.5 Hz MODE

	Calculated from small-signal model		Estimated from the time-domain responses	
	$\frac{\dot{W}_{d_{i,r}}}{2 \hat{c}_r ^2}$	$\frac{\dot{W}_{f_{i,r}}}{2 \hat{c}_r ^2}$	$\frac{\dot{W}_{d_{i,r}}}{2 \hat{c}_r ^2}$	$\frac{\dot{W}_{f_{i,r}}}{2 \hat{c}_r ^2}$
G14	0.2150	0.1642	0.2070	0.1503
G16	0.2665	0.3212	0.2904	0.3418
Sum	0.4815	0.4854	0.4974	0.4921

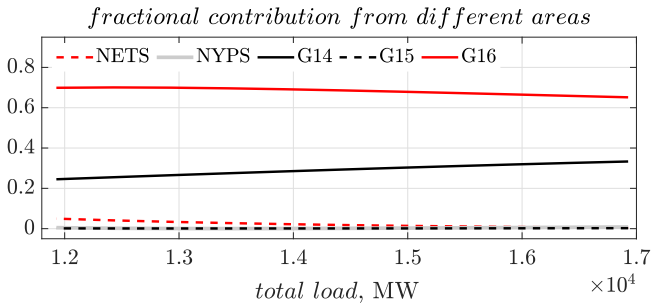


Fig. 14: Fractions in which the damping power of G16 is derived from the power dissipations in the windings of generators in NETS (G1 – G9), NYPS (G10 – G13), and G14 – G16 for the 0.50 Hz mode.

VII. CONCLUSIONS

A mathematical proof for the equality of total damping power of the system and the total power dissipation in generators was presented for multimachine systems. It was demonstrated that the equality while true when added over all generators, does not hold for individual machines. Thereafter, distribution factors were derived representing the dissipative contributions from different generators in constituting the damping power of each machine.

APPENDIX A: PHASOR NOTATION

Let the small-signal dynamics of an autonomous system be represented by the state space model $\dot{\mathbf{x}}(t) = \mathbf{A}\mathbf{x}(t)$. Next, assuming there are m oscillatory modes in the response, each due to a complex-conjugate eigenvalue pair $\lambda_r (= \sigma_r + j\omega_{d_r})$ and λ_r^* of \mathbf{A} , the time evolution of any i^{th} state variable $x_i(t)$ can be expressed as the sum of m modal constituents, as shown in eqn (32)

$$x_i(t) = \sum_{r=1}^m x_{i,r}(t) = \sum_{r=1}^m \left\{ e^{\lambda_r t} c_r \psi_{i,r} + e^{\lambda_r^* t} c_r^* \psi_{i,r}^* \right\} \quad (32)$$

where, $c_r = \phi_r^T \mathbf{x}(0)$, and ϕ_r^T and Ψ_r are respectively the left and right eigenvectors of \mathbf{A} corresponding to the eigenvalue λ_r with $\psi_{i,r}$ as the i^{th} entry of Ψ_r .

Denoting $2c_r \psi_{i,r} \triangleq \beta_{i,r} e^{j\gamma_{i,r}}$, $x_{i,r}(t)$ reduces to

$$x_{i,r}(t) = 2 \Re \left\{ e^{\lambda_r t} c_r \psi_{i,r} \right\} = \beta_{i,r} e^{\sigma_r t} \cos(\omega_{d_r} t + \gamma_{i,r}). \quad (33)$$

This sinusoidal variation is represented in the dynamic phasor (mentioned as ‘phasor’ going forward) notation using the magnitude and phase of the signal, as shown in eqn (34).

$$\vec{x}_{i,r}(t) \triangleq \beta_{i,r} e^{\sigma_r t} \angle \gamma_{i,r} = 2 c_r \psi_{i,r} e^{\sigma_r t} \quad (34)$$

$\vec{x}_{i,r}(t)$ is a phasor rotating at the modal frequency ω_{d_r} with its amplitude having an exponential decay. It represents the time evolution of $x_{i,r}(t)$. We denote \vec{x}_r as the vector of $\vec{x}_{i,r}(t)$ -s.

Next, from (33),

$$\dot{x}_{i,r}(t) = \beta_{i,r} e^{\sigma_r t} \left\{ \sigma_r \cos(\omega_{d_r} t + \gamma_{i,r}) - \omega_{d_r} \sin(\omega_{d_r} t + \gamma_{i,r}) \right\}. \quad (35)$$

Considering the mode to be poorly-damped, $|\sigma_r| \ll \omega_{d_r}$, this reduces to $\dot{x}_{i,r}(t) \approx -\beta_{i,r} e^{\sigma_r t} \omega_{d_r} \sin(\omega_{d_r} t + \gamma_{i,r})$. Therefore,

$$\vec{x}_{i,r}(t) \approx j \omega_{d_r} \vec{x}_{i,r}(t). \quad (36)$$

APPENDIX B: PROOF OF CLAIMS

Observe that, from (6), **M**, **N**, **C**, and **D** can be structured as

$$\mathbf{M} = \begin{bmatrix} \mathbf{M}_{11} & \mathbf{M}_{12} & \mathbf{M}_{13} \\ \mathbf{M}_{21} & \mathbf{M}_{22} & \mathbf{M}_{23} \\ \mathbf{M}_{31} & \mathbf{M}_{32} & \mathbf{M}_{33} \end{bmatrix} \quad \mathbf{N} = \begin{bmatrix} \mathbf{N}_{11} & \mathbf{N}_{12} \\ \mathbf{N}_{21} & \mathbf{N}_{22} \\ \mathbf{N}_{31} & \mathbf{N}_{32} \end{bmatrix} \quad (37)$$

$$\mathbf{C} = \begin{bmatrix} \mathbf{C}_{11} & \mathbf{C}_{12} & \mathbf{C}_{13} \\ \mathbf{C}_{21} & \mathbf{C}_{22} & \mathbf{C}_{23} \end{bmatrix} \quad \mathbf{D} = \begin{bmatrix} \mathbf{D}_{11} & \mathbf{D}_{12} \\ \mathbf{D}_{21} & \mathbf{D}_{22} \end{bmatrix}.$$

Following the notation that, $\mathbf{D}_{kl}(i, j)$ is the $(i, j)^{\text{th}}$ element of the $(k, l)^{\text{th}}$ submatrix \mathbf{D}_{kl} of \mathbf{D} , we may write $\forall j \neq i$

$$\mathbf{D}_{12}(i, j) = V_{j_0} \frac{\partial f_i}{\partial V_j} \Big|_0 = -V_{i_0} V_{j_0} Y_{ij} \sin(\theta_{i_0} - \theta_{j_0}) \quad (38a)$$

$$\mathbf{D}_{21}(i, j) = \frac{\partial g_i}{\partial \theta_j} \Big|_0 = V_{i_0} V_{j_0} Y_{ij} \sin(\theta_{i_0} - \theta_{j_0}) = \mathbf{D}_{12}(j, i) \quad (38b)$$

$$\mathbf{D}_{11}(i, j) = \frac{\partial f_i}{\partial \theta_j} \Big|_0 = V_{i_0} V_{j_0} Y_{ij} \cos(\theta_{i_0} - \theta_{j_0}) = \mathbf{D}_{11}(j, i) \quad (38c)$$

$$\mathbf{D}_{22}(i, j) = V_{j_0} \frac{\partial g_i}{\partial V_j} \Big|_0 = V_{i_0} V_{j_0} Y_{ij} \cos(\theta_{i_0} - \theta_{j_0}) = \mathbf{D}_{22}(j, i). \quad (38d)$$

Similarly, it can be shown that,

$$\mathbf{D}_{12}(i, i) = V_{i_0} \left. \frac{\partial f_i}{\partial V_i} \right|_0 = \left. \frac{\partial g_i}{\partial \theta_i} \right|_0 = \mathbf{D}_{21}(i, i). \quad (39)$$

Therefore, from eqns (38a), (38b), and (39), it can be inferred that $\mathbf{D}_{12}^T = \mathbf{D}_{21}$. Additionally, from eqns (38c) – (38d), $\mathbf{D}_{11}^T = \mathbf{D}_{11}$ and $\mathbf{D}_{22}^T = \mathbf{D}_{22}$. Thus,

$$\mathbf{D}^T = \begin{bmatrix} \mathbf{D}_{11} & \mathbf{D}_{12} \\ \mathbf{D}_{21} & \mathbf{D}_{22} \end{bmatrix}^T = \begin{bmatrix} \mathbf{D}_{11}^T & \mathbf{D}_{21}^T \\ \mathbf{D}_{12}^T & \mathbf{D}_{22}^T \end{bmatrix} = \mathbf{D}. \quad (40)$$

Further, \mathbf{D} being real and symmetric implies \mathbf{D}^{-1} is also real and symmetric

$$\implies \mathbf{D}^{-T} = \mathbf{D}^{-1}. \quad (41)$$

Proof of Claim (1) : Recall, $\mathbf{A} = \mathbf{M} - \mathbf{N}\mathbf{D}^{-1}\mathbf{C}$. Therefore,

$$\begin{aligned} \mathbf{A}_{33} &= \mathbf{M}_{33} - \begin{bmatrix} \mathbf{N}_{31} & \mathbf{N}_{32} \end{bmatrix} \mathbf{D}^{-1} \begin{bmatrix} \mathbf{C}_{13} \\ \mathbf{C}_{23} \end{bmatrix} \\ \implies \mathbf{A}_{33}^T &= \mathbf{M}_{33}^T - \begin{bmatrix} \mathbf{C}_{13}^T & \mathbf{C}_{23}^T \end{bmatrix} \mathbf{D}^{-T} \begin{bmatrix} \mathbf{N}_{31}^T \\ \mathbf{N}_{32}^T \end{bmatrix} \end{aligned} \quad (42)$$

From eqns (3) and (4) observe that, $\forall j \neq i$,

$$\mathbf{N}_{31}(i, j) = \left. \frac{\partial \dot{E}'_{q_i}}{\partial \theta_j} \right|_0 = 0; \quad \mathbf{C}_{13}(i, j) = \left. \frac{\partial f_i}{\partial E'_{q_j}} \right|_0 = 0; \quad (43)$$

and for elements on the principal diagonal,

$$\mathbf{N}_{31}(i, i) = \left. \frac{\partial \dot{E}'_{q_i}}{\partial \theta_i} \right|_0 = \frac{V_{i_0} \sin(\delta_{i_0} - \theta_{i_0})}{x'_{d_i}} \left(\frac{x_{d_i} - x'_{d_i}}{T'_{do_i}} \right) \quad (44a)$$

$$\mathbf{C}_{13}(i, i) = \left. \frac{\partial f_i}{\partial E_{q_i}} \right|_0 = \frac{V_{i_0} \sin(\delta_{i_0} - \theta_{i_0})}{x'_{d_i}} \quad (44b)$$

Further note, \mathbf{N}_{31} and \mathbf{C}_{13} are rectangular matrices of dimensions $\mathbb{R}^{n_g \times n}$ and $\mathbb{R}^{n \times n_g}$ respectively. Therefore, combining eqns (43) and (44) we get

$$\mathbf{P}^{-1} \mathbf{C}_{13}^T = \mathbf{N}_{31} \quad (45)$$

where, \mathbf{P} is a diagonal matrix with $\mathbf{P}(i, i) = \frac{T'_{do_i}}{x_{d_i} - x'_{d_i}}$. Similarly, from eqns (3) and (5), $\forall j \neq i$,

$$\mathbf{N}_{32}(i, j) = V_{j_0} \left. \frac{\partial \dot{E}'_{q_i}}{\partial V_j} \right|_0 = 0; \quad \mathbf{C}_{23}(i, j) = \left. \frac{\partial g_i}{\partial E'_{q_j}} \right|_0 = 0; \quad \text{and}$$

$$\mathbf{N}_{32}(i, i) = V_{i_0} \left. \frac{\partial \dot{E}'_{q_i}}{\partial V_j} \right|_0 = \frac{V_{i_0} \cos(\delta_{i_0} - \theta_{i_0})}{x'_{d_i}} \left(\frac{x_{d_i} - x'_{d_i}}{T'_{do_i}} \right)$$

$$\mathbf{C}_{23}(i, i) = \left. \frac{\partial g_i}{\partial E_{q_i}} \right|_0 = \frac{V_{i_0} \cos(\delta_{i_0} - \theta_{i_0})}{x'_{d_i}}$$

Therefore, following arguments as before,

$$\mathbf{P}^{-1} \mathbf{C}_{23}^T = \mathbf{N}_{32} \quad (46)$$

Finally, observe that $\mathbf{M}_{33} \in \mathbb{R}^{n_g \times n_g}$ with $\mathbf{M}_{33}(i, j) = \left. \frac{\partial \dot{E}'_{q_i}}{\partial \delta_j} \right|_0 = 0 \quad \forall j \neq i$. This implies \mathbf{M}_{33} is diagonal.

Using the results (41), (45) and (46), eqn (42) can be rewritten as

$$\begin{aligned} \mathbf{P}^{-1} \mathbf{A}_{33} \mathbf{P} &= \mathbf{P}^{-1} \mathbf{M}_{33} \mathbf{P} - \mathbf{P}^{-1} \begin{bmatrix} \mathbf{C}_{13}^T & \mathbf{C}_{23}^T \end{bmatrix} \mathbf{D}^{-T} \begin{bmatrix} \mathbf{N}_{31}^T \\ \mathbf{N}_{32}^T \end{bmatrix} \mathbf{P} \\ &= \mathbf{M}_{33} - \begin{bmatrix} \mathbf{N}_{31} & \mathbf{N}_{32} \end{bmatrix} \mathbf{D}^{-1} \begin{bmatrix} \mathbf{C}_{13} \\ \mathbf{C}_{23} \end{bmatrix} = \mathbf{A}_{33}. \end{aligned}$$

This concludes the proof. \square

Proof of Claim (2) : It can be seen from eqns (2) and (3) that blocks \mathbf{M}_{31} and \mathbf{M}_{23} are diagonal. Also,

$$\mathbf{M}_{31}(i, i) = \left. \frac{\partial \dot{E}'_{q_i}}{\partial \delta_i} \right|_0 = - \frac{V_{i_0} \sin(\delta_i - \theta_i)}{x'_{d_i}} \left(\frac{x_{d_i} - x'_{d_i}}{T'_{do_i}} \right) \quad (47a)$$

$$\mathbf{M}_{23}(i, i) = \left. \frac{\partial \dot{\omega}_i}{\partial E'_{q_i}} \right|_0 = - \frac{V_{i_0} \sin(\delta_i - \theta_i)}{2H_i x'_{d_i}} \omega_s \quad (47b)$$

Therefore, we may write

$$\mathbf{M}_{31}^T \mathbf{P} = \frac{2}{\omega_s} \mathbf{H} \mathbf{M}_{23} \quad (48)$$

where \mathbf{H} is diagonal with $\mathbf{H}(i, i) = H_i$.

Now, as before, for \mathbf{N} and \mathbf{C} matrices,

$$\mathbf{N}_{21}(i, j) = \left. \frac{\partial \dot{\omega}_i}{\partial \theta_j} \right|_0 = 0; \quad \mathbf{C}_{11}(i, j) = \left. \frac{\partial f_i}{\partial \delta_j} \right|_0 = 0. \quad \text{Also,}$$

$$\begin{aligned} \mathbf{N}_{21}(i, i) &= \left. \frac{\partial \dot{\omega}_i}{\partial \theta_i} \right|_0 = \frac{\omega_s E'_{q_{i_0}} V_{i_0} \cos(\delta_{i_0} - \theta_{i_0})}{2H_i x'_{d_i}} \\ &\quad - \frac{\omega_s V_{i_0}^2 \sin 2(\delta_{i_0} - \theta_{i_0})}{2H_i} \left(\frac{x_{q_i} - x'_{d_i}}{x_{q_i} x'_{d_i}} \right) \end{aligned}$$

$$\begin{aligned} \mathbf{C}_{11}(i, i) &= \left. \frac{\partial f_i}{\partial \delta_i} \right|_0 = \frac{E'_{q_{i_0}} V_{i_0} \cos(\delta_{i_0} - \theta_{i_0})}{x'_{d_i}} \\ &\quad - V_{i_0}^2 \sin 2(\delta_{i_0} - \theta_{i_0}) \left(\frac{x_{q_i} - x'_{d_i}}{x_{q_i} x'_{d_i}} \right) = \frac{2}{\omega_s} H_i \mathbf{N}_{21}(i, i) \end{aligned}$$

Combining these with the fact that, $\mathbf{N}_{21} \in \mathbb{R}^{n_g \times n}$ and $\mathbf{C}_{11} \in \mathbb{R}^{n \times n_g}$ we may write,

$$\mathbf{C}_{11}^T = \frac{2}{\omega_s} \mathbf{H} \mathbf{N}_{21}. \quad (49)$$

Similarly, it can be shown that

$$\mathbf{C}_{21}^T = \frac{2}{\omega_s} \mathbf{H} \mathbf{N}_{22}. \quad (50)$$

Now, recall $\mathbf{A} = \mathbf{M} - \mathbf{N}\mathbf{D}^{-1}\mathbf{C}$. Therefore,

$$\begin{aligned} \mathbf{A}_{31} &= \mathbf{M}_{31} - \begin{bmatrix} \mathbf{N}_{31} & \mathbf{N}_{32} \end{bmatrix} \mathbf{D}^{-1} \begin{bmatrix} \mathbf{C}_{11} \\ \mathbf{C}_{21} \end{bmatrix} \\ \implies \mathbf{A}_{31} \mathbf{P} &= \mathbf{M}_{33} \mathbf{P} - \begin{bmatrix} \mathbf{C}_{11}^T & \mathbf{C}_{21}^T \end{bmatrix} \mathbf{D}^{-T} \begin{bmatrix} \mathbf{N}_{31}^T \\ \mathbf{N}_{32}^T \end{bmatrix} \mathbf{P} \end{aligned} \quad (51)$$

Next, substituting eqns (41) and (45) – (50) in (51)

$$\begin{aligned} \mathbf{A}_{31} \mathbf{P} &= \frac{2}{\omega_s} \mathbf{H} \mathbf{M}_{23} - \frac{2}{\omega_s} \mathbf{H} \begin{bmatrix} \mathbf{N}_{21} & \mathbf{N}_{22} \end{bmatrix} \mathbf{D}^{-1} \begin{bmatrix} \mathbf{C}_{13} \\ \mathbf{C}_{23} \end{bmatrix} \\ &= \frac{2}{\omega_s} \mathbf{H} \mathbf{A}_{23} \end{aligned} \quad (52)$$

This concludes the proof. \square

Proof of Claim (3) : As before, observe from eqn (2) that \mathbf{M}_{21} is diagonal. Therefore, we may write

$$\mathbf{H} \mathbf{M}_{21} = \mathbf{M}_{21}^T \mathbf{H}. \quad (53)$$

$$\begin{aligned} \text{Also,} \quad \mathbf{A}_{21} &= \mathbf{M}_{21} - \begin{bmatrix} \mathbf{N}_{21} & \mathbf{N}_{22} \end{bmatrix} \mathbf{D}^{-1} \begin{bmatrix} \mathbf{C}_{11} \\ \mathbf{C}_{21} \end{bmatrix} \\ \implies 2 \mathbf{A}_{21} \mathbf{H} &= \mathbf{M}_{21} \mathbf{H} - \begin{bmatrix} \mathbf{C}_{11}^T & \mathbf{C}_{21}^T \end{bmatrix} \mathbf{D}^{-T} \begin{bmatrix} 2 \mathbf{N}_{21}^T \mathbf{H} \\ 2 \mathbf{N}_{22}^T \mathbf{H} \end{bmatrix} \end{aligned} \quad (54)$$

Finally, substituting eqns (41), (49), (50), and (53) in (54)

$$\begin{aligned} 2 \mathbf{A}_{21}^T \mathbf{H} &= 2 \mathbf{H} \mathbf{M}_{21} - 2 \mathbf{H} [\mathbf{N}_{21} \mathbf{N}_{22}] \mathbf{D}^{-1} \begin{bmatrix} \mathbf{C}_{11} \\ \mathbf{C}_{21} \end{bmatrix} \\ &= 2 \mathbf{H} \mathbf{A}_{21}. \end{aligned} \quad (55)$$

This concludes the proof. \square

Proof of Claim (4) : From the definition of \mathbf{K}_r and (14),

$$\begin{aligned} \mathbf{K}_r^T &= - \left\{ \frac{2}{\omega_s} \mathbf{A}_{21}^T \mathbf{H} + \mathbf{A}_{31}^T (j\omega_{d_r} \mathbf{I} - \mathbf{A}_{33}^T)^{-1} \left(\frac{2}{\omega_s} \mathbf{A}_{23}^T \mathbf{H} \right) \right\} \frac{1}{j\omega_{d_r}} \\ &= - \left\{ \frac{2}{\omega_s} \mathbf{A}_{21}^T \mathbf{H} + \mathbf{A}_{31}^T \mathbf{P} (j\omega_{d_r} \mathbf{I} - \mathbf{P}^{-1} \mathbf{A}_{33}^T \mathbf{P})^{-1} \right. \\ &\quad \left. \mathbf{P}^{-1} \left(\frac{2 \mathbf{H}}{\omega_s} \mathbf{A}_{23} \right)^T \right\} \frac{1}{j\omega_{d_r}} \end{aligned}$$

Next, using claims (1) – (3) we can re-write \mathbf{K}_r^T as

$$\mathbf{K}_r^T = - \frac{2 \mathbf{H}}{\omega_s} \left\{ \mathbf{A}_{21} + \mathbf{A}_{23} (j\omega_{d_r} \mathbf{I} - \mathbf{A}_{33})^{-1} \mathbf{A}_{31} \right\} \frac{1}{j\omega_{d_r}} = \mathbf{K}_r \quad (56)$$

Now, $\forall \mathbf{x} \in \mathbb{C}^{n_g}$, let us decompose it into its real and imaginary parts as shown: $\mathbf{x} = \mathbf{x}_1 + j\mathbf{x}_2$. Therefore,

$$\mathbf{x}^H \mathbf{K}_r \mathbf{x} = (\mathbf{x}_1^T - j\mathbf{x}_2^T) \left(\Re(\mathbf{K}_r) + j\Im(\mathbf{K}_r) \right) (\mathbf{x}_1 + j\mathbf{x}_2) \quad (57)$$

Further, using eqn (56), we can infer on the symmetry of both the real and imaginary parts of \mathbf{K}_r . Hence,

$$\mathbf{x}_1^T \Im(\mathbf{K}_r) \mathbf{x}_2 = \mathbf{x}_2^T \Im(\mathbf{K}_r) \mathbf{x}_1 \text{ and } \mathbf{x}_1^T \Re(\mathbf{K}_r) \mathbf{x}_2 = \mathbf{x}_2^T \Re(\mathbf{K}_r) \mathbf{x}_1. \quad (58)$$

This reduces the real part of eqn (57) as follows

$$\Re\{\mathbf{x}^H \mathbf{K}_r \mathbf{x}\} = \mathbf{x}_1^T \Re(\mathbf{K}_r) \mathbf{x}_1 + \mathbf{x}_2^T \Re(\mathbf{K}_r) \mathbf{x}_2. \quad (59)$$

Finally, using the real part of eqn (58)

$$\begin{aligned} \Re\{\mathbf{x}^H \mathbf{K}_r \mathbf{x}\} &= \mathbf{x}_1^T \Re(\mathbf{K}_r) \mathbf{x}_1 + \mathbf{x}_2^T \Re(\mathbf{K}_r) \mathbf{x}_2 \\ &\quad + j\mathbf{x}_1^T \Im(\mathbf{K}_r) \mathbf{x}_2 - j\mathbf{x}_2^T \Im(\mathbf{K}_r) \mathbf{x}_1 \\ &= \mathbf{x}^H \Re\{\mathbf{K}_r\} \mathbf{x}. \end{aligned} \quad (60)$$

This concludes the proof. \square

REFERENCES

- [1] R. H. Park, "Two-reaction Theory of Synchronous Machines-II," *Transactions of the American Institute of Electrical Engineers*, vol. 52, no. 2, pp. 352–354, 1933.
- [2] C. Concordia, "Synchronous Machine Damping and Synchronizing Torques," *Transactions of the American Institute of Electrical Engineers*, vol. 70, no. 1, pp. 731–737, 1951.
- [3] —, "Synchronous Machine Damping Torque at Low Speeds," *Transactions of the American Institute of Electrical Engineers*, vol. 69, no. 2, pp. 1550–1553, 1950.
- [4] R. V. Shepherd, "Synchronizing and Damping Torque Coefficients of Synchronous Machines," *Transactions of the American Institute of Electrical Engineers. Part III: Power Apparatus and Systems*, vol. 80, no. 3, pp. 180–189, 1961.
- [5] Lee A. Kilgore and E. C. Whitney, "Spring and Damping Coefficients of Synchronous Machines and Their Application," *Transactions of the American Institute of Electrical Engineers*, vol. 69, no. 1, pp. 226–230, 1950.
- [6] F. P. Demello and C. Concordia, "Concepts of Synchronous Machine Stability as Affected by Excitation Control," *IEEE Transactions on Power Apparatus and Systems*, vol. PAS-88, no. 4, pp. 316–329, Apr. 1969.
- [7] R. T. H. Alden and A. A. Shaltout, "Analysis of Damping and Synchronizing Torques Part I-A General Calculation Method," *IEEE Transactions on Power Apparatus and Systems*, vol. PAS-98, no. 5, pp. 1696–1700, Sep. 1979.
- [8] A. A. Shaltout and R. T. H. Alden, "Analysis of Damping and Synchronizing Torques Part II-Effect of Operating Conditions and Machine Parameters," *IEEE Transactions on Power Apparatus and Systems*, vol. PAS-98, no. 5, pp. 1701–1708, Sep. 1979.
- [9] A. A. Shaltout and K. A. Abu Al-Feilat, "Damping and Synchronizing Torque Computation in Multimachine Power Systems," *IEEE Transactions on Power Systems*, vol. 7, no. 1, pp. 280–286, Feb. 1992.
- [10] N. Jiang and H. Chiang, "Damping Torques of Multi-Machine Power Systems During Transient Behaviors," *IEEE Transactions on Power Systems*, vol. 29, no. 3, pp. 1186–1193, 2014.
- [11] P. W. Sauer and M. A. Pai, *Power System Dynamics and Stability*. Prentice Hall, 1998.
- [12] "Damping Representation for Power System Stability Studies," *IEEE Transactions on Power Systems*, vol. 14, no. 1, pp. 151–157, 1999.
- [13] L. Chen, Y. Min, Y. Chen, and W. Hu, "Evaluation of Generator Damping Using Oscillation Energy Dissipation and the Connection With Modal Analysis," *IEEE Transactions on Power Systems*, vol. 29, no. 3, pp. 1393–1402, 2014.
- [14] L. Chen, Y. Min, and W. Hu, "An Energy-based Method for Location of Power System Oscillation Source," *IEEE Transactions on Power Systems*, vol. 28, no. 2, pp. 828–836, May 2013.
- [15] H. Cai, S. Q. Bu, Z. Y. Peng, C. Wu, W. M. Xi, and W. C. Qi, "Consistency of Damping Torque and Energy Flow Dissipation Coefficient in Oscillation Stability Analysis," in *2018 International Conference on Power System Technology (POWERCON)*, 2018, pp. 2284–2290.
- [16] D. J. Trudnowski, J. W. Pierre, N. Zhou, J. F. Hauer, and M. Parashar, "Performance of Three Mode-Meter Block-Processing Algorithms for Automated Dynamic Stability Assessment," *IEEE Transactions on Power Systems*, vol. 23, no. 2, pp. 680–690, 2008.
- [17] P. Kundur, *Power System Stability and Control*. McGraw-Hill, 1994.
- [18] X. T. Jiang, J. H. Chow, and F. Wilches-Bernal, "A synchrophasor measurement based method for assessing damping torque contributions from power system stabilizers," in *2015 IEEE Eindhoven PowerTech*, 2015, pp. 1–6.
- [19] N. R. Chaudhuri, "Wide-area Monitoring and Control of Future Smart Grids," Ph.D. dissertation, Imperial College, London, U.K., 2011.
- [20] L. Dosiek and J. W. Pierre, "Estimating Electromechanical Modes and Mode Shapes using the Multichannel ARMAX model," *IEEE Transactions on Power Systems*, vol. 28, no. 2, pp. 1950–1959, 2013.